HYDRAULIC FLOW THROUGH SATURATED CLAYS

by

HAROLD W. OLSEN[1]

Soil Engineering Division, Department of Civil Engineering,
Massachusetts Institute of Technology, Cambridge, Massachusetts

ABSTRACT

The factors: (1) possible violations of Darcy's law, (2) electrokinetic coupling, (3) high viscosity, (4) tortuous flow paths, and (5) unequal pore sizes have been suggested as possible explanations for the differences between hydraulic flow rates in liquid-saturated clays and sands. The effects of these factors on hydraulic flow rates through saturated clays were investigated.

Hydraulic flow rates, electrical conductivities, and streaming potentials were measured on natural, sodium, and calcium samples of kaolinite, illite and Boston blue clay. Data were taken after increments of one-dimensional consolidation and rebound over the pressure range from one-sixteenth to 256 atm.

The influences of electrokinetic coupling on the hydraulic flow rates were calculated from irreversible thermodynamic relationships together with the hydraulic and electrical data. The other factors were studied by examining the extent to which each factor explains the discrepancies between measured flow rates and those predicted from Darcy's law and the Kozeny–Carman equation.

The results show that: (1) the possible violations of Darcy's law and electrokinetic coupling are insignificant, (2) high viscosity and/or tortuous flow paths fail completely to account for the discrepancies between measured and predicted flow rates in clays, and (3) unequal pore sizes can explain all the discrepancies.

INTRODUCTION

Hydraulic flow rates through liquid-saturated porous media can be predicted closely from eq. (1) provided that the media particles are approximately (1) equidimensional, (2) uniform, (3) larger than 1 μ and (4) small enough so that the liquid flow is laminar (Carman, 1956; London, 1952).

$$q = \frac{1}{\eta}\left(\frac{P}{L}\right)K, \tag{1}$$

[1] Present address, U.S. Geol. Survey, Ground Water Branch, Washington 25, D.C.

https://doi.org/10.1346/CCMN.1960.0090108 Published online by Cambridge University Press

where

$$K = \frac{1}{kT^2 S_0^2} \frac{n^3}{(1-n)^2},$$

q = hydraulic flow rate,

η = viscosity,

k = pore shape factor ≈ 2.5,

T = tortuosity $\approx \sqrt{2}$,

S_0 = specific surface area per unit volume of particles,

n = porosity,

P/L = hydraulic pressure gradient.

Equation (1) consists of Darcy's law and the well known Kozeny–Carman equation which is one of the most thoroughly tested correlations between permeability and the physical properties for porous media. The principal assumptions underlying eq. (1) are that (1) Darcy's law is valid, (2) viscous flow obeys Poiseuille's law, (3) the tortuosity of the flow channels is a constant and approximately equal to $\sqrt{2}$, and (4) the flow channels or pores are equal in size.

The inadequacy of eq. (1) for saturated clays has long been recognized. It fails to predict the magnitudes and the porosity dependencies of hydraulic flow rates, and it further fails to account for their dependence on the chemical compositions of the clay and permeant and on the stress history (Terzaghi, 1925; Macey, 1942; Michaels and Lin, 1954; Lambe, 1954; and others).

Four principal factors have been suggested as possible explanations for the failure of eq. 1 in saturated clays: (1) electrokinetic coupling (Elton, 1948); (2) high viscosity (Terzaghi, 1925; Macey, 1942); (3) tortuous flow paths (Lambe, 1958); and (4) unequal pore sizes (Michaels and Lin, 1954).

Electrokinetic Coupling

Electrokinetic coupling is the interaction that occurs between viscous and electrical flows in membrane materials such as clays. For the specific case when liquid is forced through a clay by a hydraulic gradient, the coupling gives rise to an induced electrical gradient that causes an osmotic flow opposite to the flow caused by the hydraulic gradient. The net result of this process is a reduction of the flow rate below that predicted from Poiseuille's law.

High Viscosity

Many investigators believe that unbalanced clay particle surface forces influence the adjacent liquid so that it exhibits a viscosity that exceeds the bulk liquid value by an amount that decreases with distance from the clay particle surfaces. If such high viscosity exists in an appreciable volume

of the clay pore space, flow rates will be less than those predicted from Poiseuille's law which assumes that the pore liquid viscosity is a constant throughout and equal to the bulk liquid value.

Tortuous Flow Paths

It has been suggested that in clays, owing to the anisometric shapes and orientations of clay particles, the liquid flow paths may be far more tortuous than the constant value of $\sqrt{2}$ assumed by the Kozeny–Carman equation.

Unequal Pore Sizes

It has been suggested that the primary particles in a clay mass may be arranged in groups such as aggregates, packets or domains (Michaels, 1959; Quirk, 1959), and that the total porosity may be distributed among inter- and intra-group components. If some such grouping arrangement of particles exists in clays, the flow channels surrounding particle groups probably will be considerably larger than those passing through the groups and between the individual particles.

In addition to the above factors, errors will occur in eq. (1) if, as recent evidence suggests, Darcy's law is not universally valid in saturated clays. Recent data obtained by the Swedish Geotechnical Institute (Hansbo, 1960) show that, for three of the four natural undisturbed clay samples tested, the flow rate versus hydraulic gradient relationships deviated from linearity at small hydraulic gradients.

The extent to which each of the above factors can account for the failure of eq. (1) in clays was investigated. An experimental test program was conducted with the primary purpose of defining the discrepancies that occur between measured hydraulic flow rates and those predicted from eq. (1) in a variety of saturated clays and over a wide range of experimental conditions. Then, analyses were made of the extent to which these discrepancies can be explained by each of the factors.

This paper is a contribution from the M.I.T. Soil Engineering Division. The investigation was conducted as a part of the author's doctorate program under the supervision of Professor T. William Lambe. The author gratefully acknowledges the advice and constructive criticism offered by Professor Lambe, Dr. R. T. Martin, and several other members of the Soil Engineering Division Staff; and Professor A. S. Michaels of the M.I.T. Chemical Engineering Department. He further acknowledges the assistance of Professor T. Madden and Dr. D. Marshall of the M.I.T. Geophysics Laboratory, who introduced the author to irreversible thermodynamics and aided in the development of the electrical measurement system.

EXPERIMENTAL INVESTIGATION

Experimental data were obtained on the clays listed in Table 1. Most of the samples were permeated with their equilibrium dialyzate solutions of 10^{-1} to 10^{-4} N sodium and calcium chloride. The remaining samples of natural and sodium kaolinite were mixed and permeated with distilled water and with various concentrations of the highly active dispersant, sodium tetraphosphate.

TABLE 1.—CLAY PROPERTIES

Clay	Surface Area (m^2/g)[1]	Glycol Retention, (mg/g)
Natural kaolinite	11	—
Sodium kaolinite	11	3.8
Calcium kaolinite	11	8.0
Sodium illite[2]	100	34.5
Sodium Boston blue clay[3]	55	9.8
Calcium Boston blue clay[3]	55	29.0

[1] From nitrogen adsorption and glycol retention measurements.

[2] Minus 20 μ fraction of Fithian illite, containing about 1 percent organic matter.

[3] Minus 1 μ fraction, consisting of illite and chlorite with 10–20 percent quartz and feldspars.

Hydraulic flow rates, electrical conductivities, and streaming potentials were measured in one dimensional consolidation–permeation tests. The test cell is shown in Fig. 1. Measurements were taken after increments of consolidation and rebound over the pressure range from one-sixteenth to 256 atm.

To insure complete liquid saturation of the samples they were placed in the test cell as slurries that were concentrated just enough to prevent segregation of particle sizes. The loose material was gradually consolidated with seepage pressure and then with small load increments up to a consolidation pressure of one-sixteenth atm, at which point the test cycle was begun.

Upward permeation of a sample was produced by placing a hydrostatic head of the permeant (not exceeding 10 percent of the consolidation pressure) in a vertical calibrated standpipe that was attached to the base of the test cell. Flow rates were computed from the measured dimensions of the samples, the mean total flow rates, and the log mean hydrostatic heads.

For the electrical measurements the cell was provided with a four-electrode system consisting of a pair of electrodes on the inner or sample sides of the porous stones and a second pair of electrodes on the outer sides of the stones. Leads from the electrodes were sealed with a fast-drying

resin in small holes drilled through the lucite test cell. The electrodes and leads were silver gauze and silver wire, coated electrolytically with silver chloride.

Streaming potentials were measured[1] with a Leeds and Northrup type K potentiometer attached to the inner electrodes. The slope of the streaming

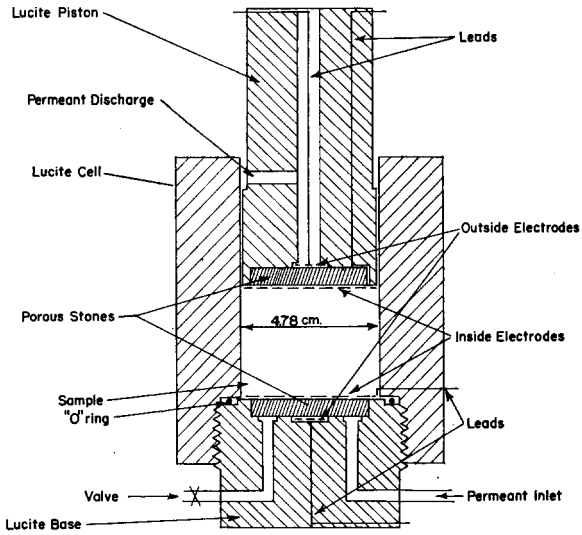

FIGURE 1.—Consolidation permeation test unit, approximately to scale.

potential–hydraulic gradient relationship was obtained from measurements of streaming potentials over a range of hydraulic permeation pressure gradients.

Conductivities were determined from measurements of the voltage drops across the inner electrodes and across a known resistance in the series circuit during the passage of D.C. current through the sample via the outer electrodes. Dry cells were used for the voltage source, and the voltage drops were measured with a Ballantine A.C. voltmeter together with an A.C.–D.C. interrupter.

[1] Periodic checks were made to determine whether the measured potentials contained, in addition to the streaming potentials, components of electrode potentials. The latter will arise if the clay samples exert a filtering action on the permeant salts. The checks consisted of measuring induced potentials before and after flushing the bottom porous stone with permeant liquid. As the flushing produced no significant changes in induced potentials, it was concluded that the streaming potentials alone were being measured by this technique.

https://doi.org/10.1346/CCMN.1960.0090108 Published online by Cambridge University Press

RESULTS

Typical Results

Typical results are presented in Figs. 2, 3 and 4 which show the principal features of the behavior of hydraulic flow rates in saturated clays. For kaolinite, illite, and Boston blue clay, respectively, the figures present predicted and measured flow rates per unit gradient plotted *vs.* porosity.

The figures contain the results from two samples of each clay: those samples that, among all the samples tested, had the largest differences in flow rates at any given porosity. The results for each sample are labeled with its clay type and permeant composition.

The predicted flow rates per unit gradient were computed from eq. (1), using specific surface area values for each clay that were obtained from nitrogen adsorption and glycol retention measurements.

The measured flow rates per unit gradient were calculated from the data taken during the consolidation and rebound cycles of the consolidation permea-

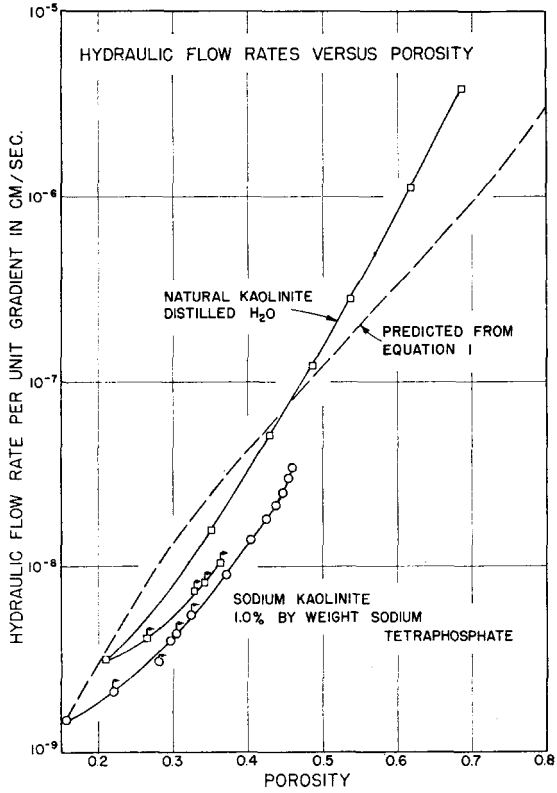

FIGURE 2.—Hydraulic flow rates versus porosity: kaolinite.

https://doi.org/10.1346/CCMN.1960.0090108 Published online by Cambridge University Press

tion tests. They are the mean total flow rates per unit area of sample divided by the log-mean hydrostatic head. The data from rebound cycles are indicated with arrows pointing in the direction of increasing porosity.

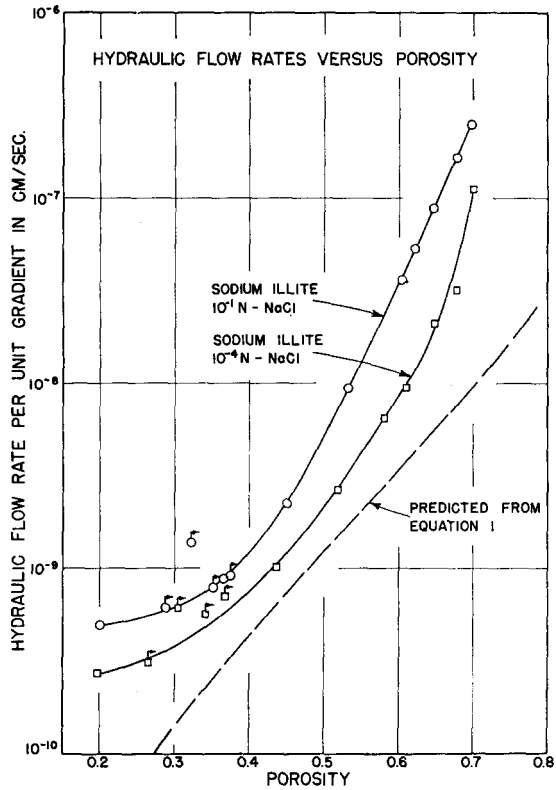

FIGURE 3. – Hydraulic flow rates versus porosity: illite.

Discrepancies Between Measured and Predicted Flow Rates

The analyses in the following sections of this paper deal with the possible causes for the discrepancies that occur between the measured and predicted flow rates shown in Figs. 2, 3 and 4. In particular, the analyses are concerned with the variations of these discrepancies with porosity, clay type, and the chemical compositions of the clay and permeant. The discrepancies are more clearly shown in Figs. 5 and 6 where the ratios of measured to predicted flow rates have been plotted *vs.* porosity. The compression cycle results are plotted in Fig. 5; the rebound results, in Fig. 6.

The results in Fig. 5, for porosities greater than about 0.5, show trends that are similar to results that have been presented by previous investi-

https://doi.org/10.1346/CCMN.1960.0090108 Published online by Cambridge University Press

gators; namely, that measured flow rates decrease more rapidly with decreasing porosity than those predicted, and that measured flow [rates

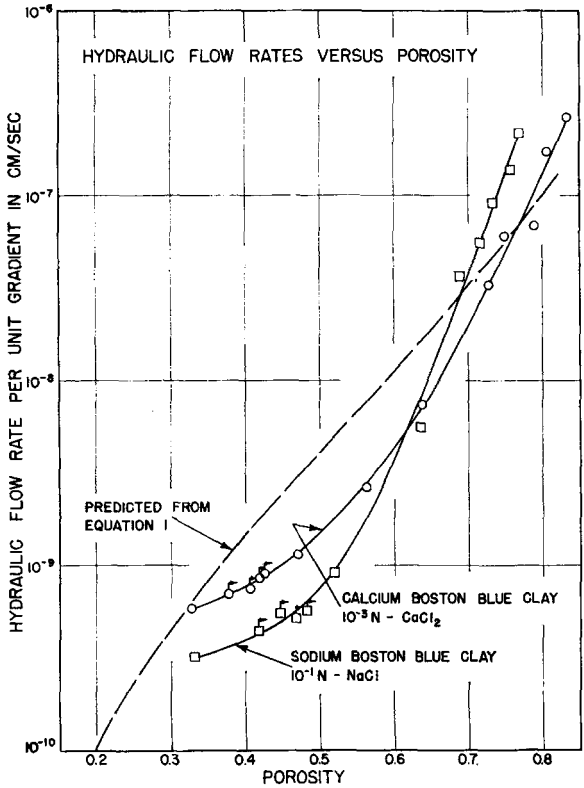

FIGURE 4.—Hydraulic flow rates versus porosity: Boston blue clay.

decrease with increasing dispersion of a clay at constant porosity (Terzaghi, 1925; Macey, 1942; Lambe, 1954; Quirk and Schofield, 1955).

The results also show trends which (to the writer's knowledge) have not been reported in the literature. During compression at porosities less than about 0.4 (Fig. 5), measured flow rates decrease less rapidly with decreasing porosity than those predicted; during rebound (Fig. 6), measured flow rates increase less rapidly with increasing porosity than those predicted; and measured flow rates are often considerably higher than those predicted.

DISCUSSION

The factors (1) possible violations of Darcy's law, (2) electrokinetic coupling, (3) high viscosity, (4) tortuous flow paths, and (5) unequal pore

https://doi.org/10.1346/CCMN.1960.0090108 Published online by Cambridge University Press

sizes, are considered separately in this discussion. The extent to which each factor can explain the actual discrepancies[1] is examined.

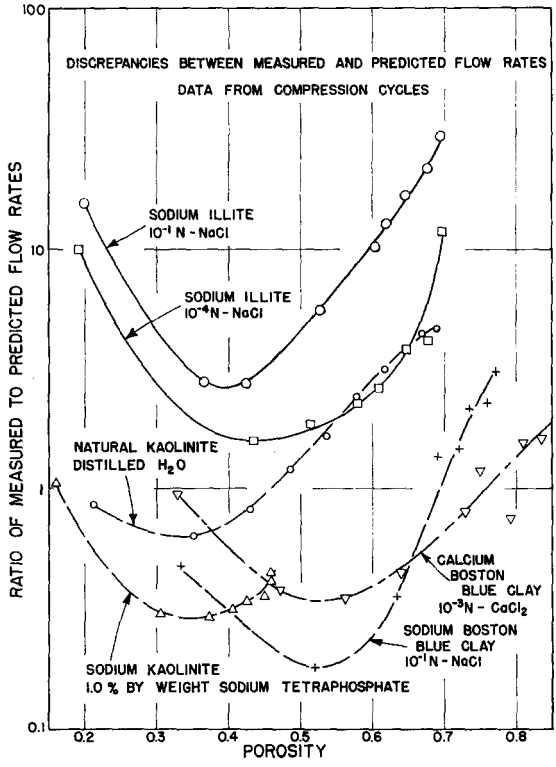

FIGURE 5.—Discrepancies between measured and predicted flow rates; data from compression cycles.

Darcy's Law

Darcy's law asserts that the rate of flow through a porous medium is directly proportional to the applied hydraulic gradient. Two concepts are implied in this assertion. First, the flow rate versus hydraulic gradient relationship is linear. Second, the linear relationship passes through the origin.

With regard to the first concept, the linearity of flow rates versus hydraulic gradients has been reported by numerous investigators. For example, Terzaghi (1925) and Macey (1942) reported linearity for the clays used in their classic permeability studies; Michaels and Lin (1954) referred to the evidence collected by Muskat that shows linearity for kaolinite; and

[1] The discrepancies between measured and predicted flow rates that were obtained in the experimental investigation are hereafter referred to as the "actual discrepancies."

Low (1960) presented data showing linearity for Na-montmorillonite. For the clays tested in this investigation, linearity was found from periodic checks made during the consolidation permeation tests over the range of gradients used for permeation, and also from a test on Na-kaolinite that was made over an extremely wide range of gradients. The results of this last test are presented in Fig. 7.

Apparently contradictory evidence has been reported by Von Englehardt and Tunn (1955) for sandstones, and by Lutz and Kemper (1959) for clays. Their results show considerable deviations from linearity between flow rates and hydraulic gradients. These results, however, were not considered significant to this discussion, since the deviations appear to be explainable by factors other than the failure of Darcy's law in the individual pores. The experimental conditions were such that the deviations could have resulted from sample volume changes, variations in the degree of saturation, and the migration and rearrangement of fines.

Data reported by Hansbo (1960) indicate, however, that the second con-

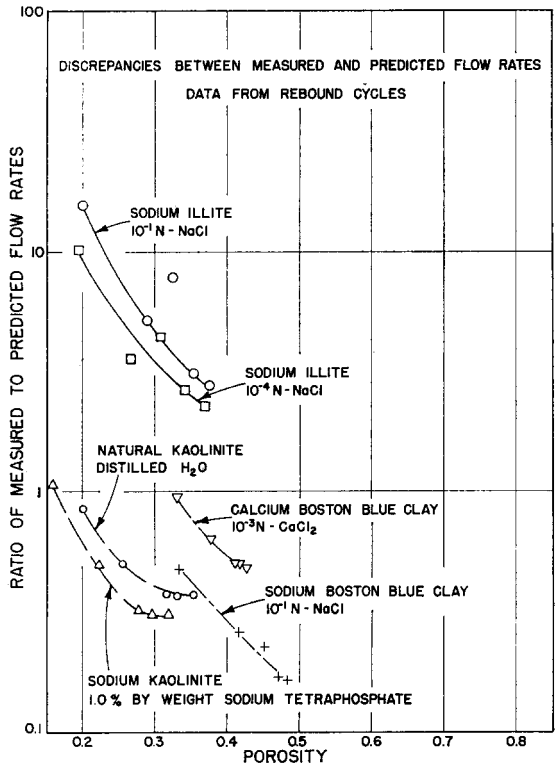

FIGURE 6.—Discrepancies between measured and predicted flow rates; data from rebound cycles.

https://doi.org/10.1346/CCMN.1960.0090108 Published online by Cambridge University Press

cept may not be universally valid for clays. Darcy's law was tested on four natural undisturbed clay samples in an extremely sensitive flow rate measuring system under carefully controlled experimental conditions. For hydraulic gradients greater than 10, the results show linearity of flow rates and gradients in all the samples. For gradients less than 10, the flow rate *vs.* gradient relationships deviated from linearity in three of the four samples. The results are illustrated in Fig. 8.

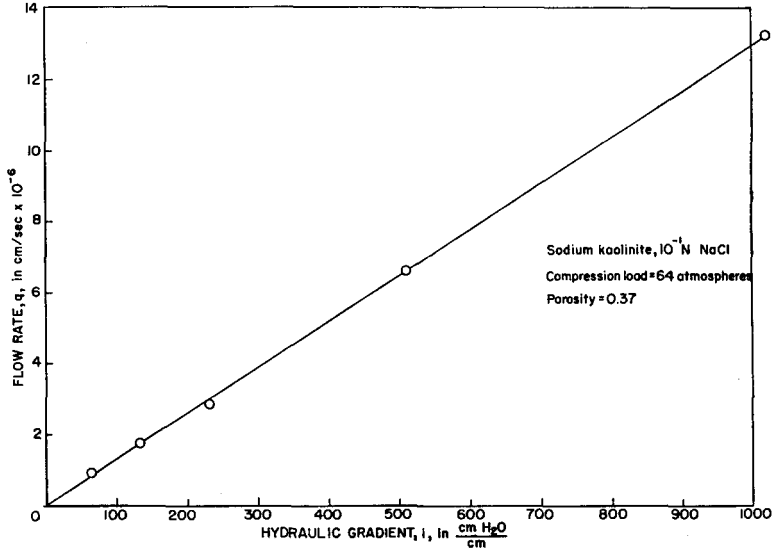

FIGURE 7.—Hydraulic flow rates versus hydraulic gradient.

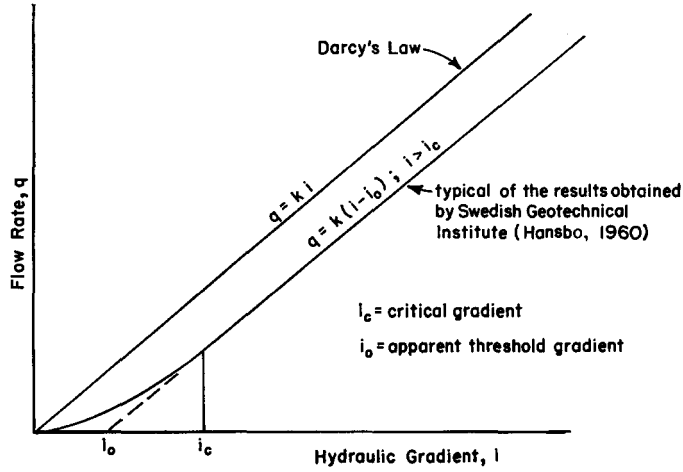

FIGURE 8.—Hydraulic flow rates versus hydraulic gradient.

https://doi.org/10.1346/CCMN.1960.0090108 Published online by Cambridge University Press

The above evidence indicates that the assumption of linearity between flow rates and hydraulic gradient is, in all probability, generally valid for saturated clays when the gradients are not small. For some clays, however, there may be critical gradients below which flow rates cease to be linear with hydraulic gradients.

Whether or not such critical gradients existed in the clays used in the experimental investigation cannot be resolved from the data obtained. Although no deviations from Darcy's law were observed, the evidence was not taken with the precision required to rule out the possibility that deviation from linearity, on the order of magnitude of those in the Swedish data, might have occurred. In the following, the extent to which these possible violations of Darcy's law can explain the actual discrepancies is examined.

The discrepancies from eq. (1) that such possible errors in Darcy's law could cause may be expressed as the ratio, q_1/q where q_1 is the flow rate through a system in which the assumptions of eq. (1) apply except that for Darcy's law, and q is eq. (1).

$$q_1 = \frac{\gamma}{\eta} K (i - i_0), \tag{2}$$

where γ = liquid density,

i = applied hydraulic gradient $= \dfrac{P}{\gamma L}$,

i_0 = apparent threshold gradient (defined in Fig. 8)

$$\frac{q_1}{q} = \frac{i - i_0}{i}. \tag{3}$$

The gradients used in the experimental investigation were, except for very low consolidation pressures, greater than 50 and less than 200. The apparent threshold gradients, i_0, could have been of the order of magnitude of those in the Swedish data, which varied from 0 to 3. These values lead to estimated discrepancy ratios, q_1/q, that range from 1.0 to 0.94.

In comparison with the actual discrepancy ratios, which for a given clay permeant system varied on the order of a factor of 10 (see Fig. 5), the estimated possible discrepancies are insignificant. Hence, the actual discrepancies cannot be explained by the possible violations of Darcy's law.

Electrokinetic Coupling

The influences of electrokinetic coupling on the measured flow rates were computed from irreversible thermodynamic relationships together with the experimental data on hydraulic flow rates, electrical conductivities, and streaming potentials.

https://doi.org/10.1346/CCMN.1960.0090108 Published online by Cambridge University Press

The irreversible thermodynamic relationships that apply to the steady state and coupled processes of viscous and electrical flows in liquid saturated clay systems are, according to Guggenheim (1957),

$$q = L_{11}(P/L) + L_{12}(E/L), \tag{4a}$$

$$i = L_{21}(P/L) + L_{22}(E/L), \tag{4b}$$

$$L_{12} = L_{21}, \tag{4c}$$

where: E/L = electrical potential gradient,
i = electrical current flow rate,
$L_{11}, L_{12}, L_{21}, L_{22}$ = phenomenological coefficients.

Equations (4a), (4b) and (4c) were derived from Onsager's general phenomenological relationships for irreversible phenomena. For clays the general relationships are applicable to the steady state and interrelated processes of viscous, current, heat, and diffusion flows that may be caused by one or more of the gradients of hydraulic pressure, electrical potential, ionic concentration, and temperature (deGroot, 1959; Denbigh, 1951). When thermal and ionic gradients are absent across a system, the general relationships simplify to eqs. (4).

The extra unknown in eqs. (4) was provided for by obtaining the data under two sets of experimental conditions. The flow rate and streaming potential measurements were taken while the samples were acted on only by externally applied hydraulic gradients. For the conductivity measurements, electrical potential gradients were applied and hydraulic gradients were maintained equal to zero.

When liquid flow is produced by a hydraulic gradient, eq. (4a) expresses the flow rate in terms of the applied hydraulic gradient, P/L, and the induced streaming potential gradient, E/L. If the influence of electrokinetic coupling is negligible or absent, the streaming potential term vanishes and eq. (4a) reduces to a form of Darcy's law, eq. (5),

$$q = L_{11}\frac{P}{L}. \tag{5}$$

The influences of electrokinetic coupling on hydraulic flow rates may be expressed by the difference between eq. (4a) and (5). It will be convenient to express this difference relative to eq. (5), or in other words, relative to the flow rate that would exist in the absence of coupling,

$$\frac{q_2 - q'}{q'} = \frac{L_{12}}{L_{11}}\left(\frac{E}{P}\right), \tag{6}$$

where q_2 = flow rate from eq. (4a),
q' = flow rate from eq. (5).

The coupling influences were computed from eq. (6) for all the hydraulic flow rates measured in the consolidation permeation tests, after the values for the phenomenological coefficients had been determined. The coefficients

were calculated from eqs. (4) together with the experimentally measured hydraulic flow rates, electrical conductivities, and streaming potentials.

The coupling influence values varied considerably with consolidation pressure, and they passed through or reached maxima usually in the high pressure range of the tests. The maximum values for all the clay–permeant systems are listed in Table 2. The values express, in percent, the maximum retardation in flow rate due to electrokinetic coupling, relative to the flow rate that would exist in the absence of coupling.

Table 2 shows that no values exceed 3.4 percent and usually they were less than 1.0 percent. The order of magnitude of these results is completely insignificant in comparison with the actual discrepancies which, as can be seen in Figs. 5 and 6, vary over a range of several hundred percent. The influences of electrokinetic coupling cannot even begin to account for the actual discrepancies and the failure of eq. (1) in clays.

TABLE 2.—INFLUENCES OF ELECTROKINETIC COUPLING

Clay	Permeant	Influence of Electrokinetic coupling (percent)[1]
Natural kaolinite	Distilled H_2O	0.22
Sodium kaolinite	10^{-1} N NaCl	0.15
Sodium kaolinite	10^{-3} N NaCl	1.16
Sodium kaolinite	10^{-4} N NaCl	2.52
Sodium kaolinite	0.02% sodium tetraphosphate (by weight)	2.22
Sodium kaolinite	1.0% sodium tetraphosphate (by weight)	1.40
Calcium kaolinite	10^{-1} N $CaCl_2$	0.001
Calcium kaolinite	10^{-3} N $CaCl_2$	0.012
Sodium illite	10^{-1} N NaCl	0.81
Sodium illite	10^{-4} N NaCl	3.33
Sodium Boston blue clay	10^{-1} N NaCl	0.13
Calcium Boston blue clay	10^{-1} N $CaCl_2$	0.05
Calcium Boston blue clay	10^{-3} N $CaCl_2$	0.98

[1] Retardation of flow rate relative to that flow rate which would exist in the absence of coupling.

High Viscosity

An estimate was made of the discrepancies from eq. (1) that could arise owing to the sole influence of high viscosity. These estimated possible discrepancies are compared with the actual discrepancies. With this comparison, the extent to which high viscosity can explain the actual discrepancies is examined.

Estimated possible discrepancies.—It will be convenient to have the possible discrepancies due to high viscosity defined by the ratio, q_3/q; where q_3 is the flow rate through a porous medium of a liquid having high viscosity, and q is the flow rate predicted from eq. (1).

The possible discrepancies were estimated for the assumed condition that high viscosity is the sole cause for the failure of eq. (1) in clays. A basis for estimating the possible discrepancies was obtained by deriving (Olsen, 1961) a relationship for the flow rate, q_3, using the assumptions in eq. 1 except that for viscosity.

Equation (1) assumes that the pore liquid viscosity is constant throughout and equal to the bulk liquid value. The assumption used here for high viscosity is that the liquid in the zone between the pore wall and a distance t from the wall is infinitely viscous, and the liquid in the pore center and beyond the distance t from the wall has a constant viscosity that is equal to the bulk liquid value. This assumption, in other words, states that the influence of high viscosity on flow rates is equivalent to the influence of a rigid film of liquid of thickness t adjacent to the pore wall.

A more reasonable concept of abnormal viscosity probably would be one in which viscosity decreases exponentially with distance from a clay particle surface. Nevertheless, the use of the simpler rigid film concept in this analysis can be justified on the grounds that both concepts lead to similar violations of Poiseuille's law. According to both concepts, the flow rate through a capillary tube will be less than predicted from Poiseuille's law by an amount that increases with (1) decreasing tube diameters, and (2) the distance the excess viscosity extends into the capillary tube.

The derived relationship for the flow rate, q_3, is given in eq. 7. The equation is expressed as the ratio, q_3/q,

$$\frac{q_3}{q} = (1 + \beta),$$

$$\text{where } \beta = \frac{3}{2}(S_0 t)\left(\frac{1-n}{n}\right)\left[\frac{S_0 t}{6}\left(\frac{1-n}{n}\right) - 1\right], \tag{7}$$

$$q = \text{eq. (1)}.$$

Hence eq. (7) is also an expression for the estimated possible discrepancies due to high viscosity.

Equation (7) was used to compute estimated possible discrepancies for the coarsest and finest clays used in this investigation. For each clay, discrepancies were computed for several arbitrary values of the rigid liquid film thickness, t. The results are presented in Fig. 9.

For the interpretation of Fig. 9, it is necessary to have an assumption concerning the variation of the immobile liquid film thickness, t, with porosity in a particular clay–permeant system. The assumption that t remains

https://doi.org/10.1346/CCMN.1960.0090108 Published online by Cambridge University Press

approximately constant with porosity appears reasonable in light of the following.

It is generally believed that, if high viscosity exists in clay pore liquid, the causes are the unbalanced particle surface forces that influence the molecular structure of the adjacent liquid. The magnitude of these influences, and the distance they extend into the pore liquid, probably do not vary appreciably with factors other than the clay particle surface charge density and the chemical compositions of the clay and permeant.

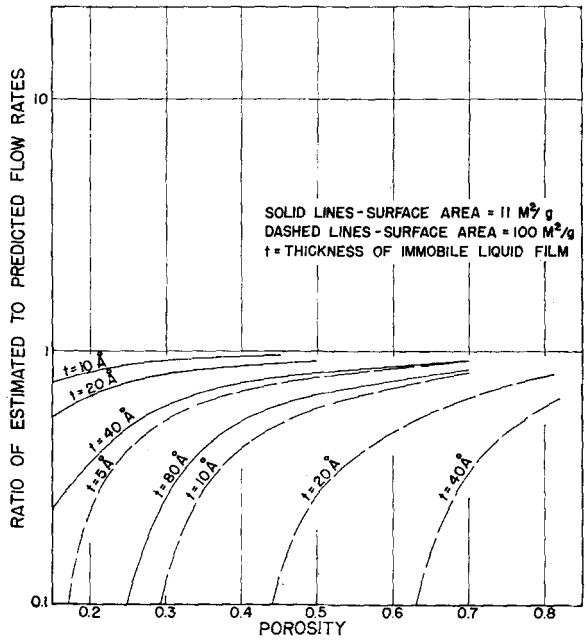

FIGURE 9.—Possible discrepancies due to high viscosity.

Comparison of the possible and actual discrepancies.—A comparison of Fig. 9 with Figs. 5 and 6 shows that most of the actual discrepancies disagree rather than agree with those possible owing to the sole influence of high viscosity.

(a) Fig. 5 shows that a large portion of the actual discrepancy ratios have values considerably greater than unity; thus measured flow rates are often higher than those predicted from eq. (1). Fig. 9 shows that high viscosity cannot account for discrepancy ratios greater than unity.

(b) Fig. 5 shows that during compression at porosities less than about 0.4–0.5, the actual discrepancy ratio increases with decreasing porosity. This means that measured flow rates are decreasing less rapidly with poro-

https://doi.org/10.1346/CCMN.1960.0090108 Published online by Cambridge University Press

sity than those predicted from eq. (1). Fig. 9 shows that high viscosity is totally unable to account for this increasing discrepancy ratio with decreasing porosity. High viscosity predicts the exact opposite behavior.

(c) Fig. 6 shows that during rebound the actual discrepancy ratio decreases with increasing porosity. This behavior means that measured flow rates increase more slowly with increasing porosity than predicted by eq. (1). Again, high viscosity is totally unable to account for this behavior. Fig. 9 shows that high viscosity would cause the reverse.

(d) Finally, Fig. 9 predicts that for illite (assuming $t = 10$ Å) the measured flow rate should become essentially zero at a porosity of about 0.25. Fig. 5 shows, however, that the flow rates for illite at a porosity of 0.2 are of the order of 10 times that value predicted by eq. (1).

The foregoing comparison[1] clearly shows that the actual discrepancies cannot be explained by the sole influence of high viscosity.

One aspect of the actual discrepancies in Fig. 5 does appear similar to the corresponding aspect of the estimated possible discrepancies in Fig. 9. That is, during compression at porosities greater than about 0.5, the actual and the possible discrepancy ratios both decrease with decreasing porosity. Even though the actual discrepancies cannot be explained solely with high viscosity, the question remains whether high viscosity may be a contributing factor.

The fact that during compression at porosities greater than about 0.5, measured flow rates decrease more rapidly than those predicted from eq. (1) and high viscosity predicts the same, has been pointed out by several previous investigators (Terzaghi, 1925; Macey, 1942). The agreement between the actual and possible discrepancies in this case is the essential basis of their contention that the "abnormal" permeability behavior of clay is caused by abnormal or high viscosity.

Two considerations have led the writer to the conclusion that high viscosity is not causing this aspect of the actual discrepancies, even though they are similar to the analogous possible discrepancies predicted by high viscosity.

(a) Fig. 9 shows that during compression and the consequent decreasing porosities, high viscosity should cause the discrepancy ratio to decrease at a rate that increases approximately exponentially with decreasing porosity. Since, however, the actual discrepancies at low porosities cannot in any way be attributed to high viscosity, it seems most unlikely that high viscosity is contributing to the discrepancies at the high porosities.

[1] Items (b) and (c) are the most important arguments in the comparison since they depend only on the shapes of the discrepancy curves in Figs. 5 and 6. Items (a) and (d) depend on the discrepancy magnitudes which vary somewhat depending on the values one chooses for the constants in eq. (1). If different values were chosen, the curves would be shifted up or down; their shapes, however, would remain constant.

(b) If it is assumed that the decrease in actual discrepancy ratio with decreasing porosity is caused by high viscosity, the consequent thicknesses of immobile water films are on the order of 300 Å for kaolinite, 150 Å for Boston blue clay, and 30 Å for illite. A 10-fold difference between kaolinite and illite seems highly unreasonable.

In summary, the foregoing comparison has shown that virtually none of the actual discrepancies can be explained by high viscosity. This result does not, however, exclude the possibility that high viscosity exists near particle surfaces. If high viscosity is present, its effects on hydraulic flow rates are being masked by other factors.

Tortuous Flow Paths

An estimate was made of the discrepancies from eq. (1) that could arise owing to the sole influence of tortuous flow paths. These estimated dis-

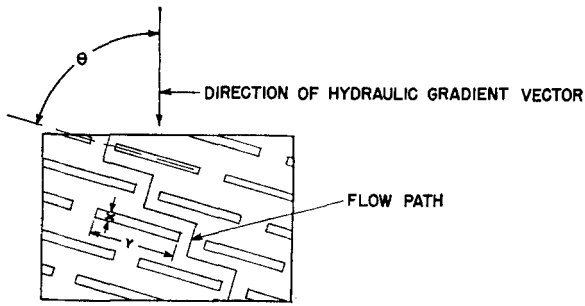

FIGURE 10.—Model and parameters for tortuous flow paths. θ = average degree of particle orientation; T = tortuosity-flow path length per unit distance along the hydraulic gradient vector; R = particle axial ratio = X/Y.

crepancies are compared with the actual discrepancies. With this comparison, the extent to which the actual discrepancies can be explained by tortuous flow paths is examined.

Estimated possible discrepancies.—The possible discrepancies due to tortuous flow paths are defined herein by the ratio, q_4/q; where q_4 is the flow rate through a medium having highly tortuous flow paths, and q is the flow rate predicted from eq. (1).

The possible discrepancies were estimated for the assumed condition that tortuous flow paths are the sole cause for the failure of eq. (1) in clays. A basis for the estimate was obtained by deriving a relationship for the flow rate, q_4, through the model of anisometric and partially oriented particles shown in Fig. 10 (Olsen, 1961). The model considers that the clay particles, of axial ratio R, are preferentially oriented to a degree θ with

https://doi.org/10.1346/CCMN.1960.0090108 Published online by Cambridge University Press

respect to the direction of the hydraulic gradient vector. The relationship for q_4 is identical to eq. (1) except that tortuosity is a variable depending on R, θ, and the void ratio, e.

$$T' = (1 + \delta) \sin\theta, \tag{8}$$

where

$$\delta = \frac{\frac{1}{2}\left[\sqrt{\left\{\left(1+\frac{1}{R}\right)^2+\frac{4e}{R}\right\}}-\left(\frac{1}{R}\right)\right]}{\sqrt{\left\{\left(1+\frac{1}{R}\right)^2+\frac{4e}{R}\right\}}+\left(1-\frac{1}{R}\right)}.$$

Using eq. (8) together with eq. (1), a relationship is immediately obtained for the possible discrepancies from eq. (1).

$$\frac{q_4}{q} = \left(\frac{T}{T'}\right)^2, \tag{9}$$

where $T = \sqrt{2}$,
$T' =$ eq. (8).

Fig. 11 shows the estimated possible discrepancies that were computed from eq. (9) for a range of particle axial ratios and degrees of particle alignment that might exist in clays. For the interpretation of Fig. 11 it will

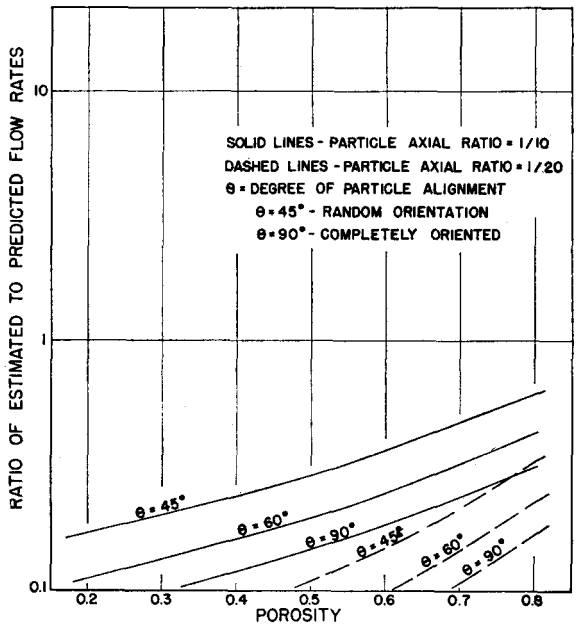

FIGURE 11.—Possible discrepancies due to tortuous flow paths.

https://doi.org/10.1346/CCMN.1960.0090108 Published online by Cambridge University Press

suffice to note that the degree of particle orientation in a clay increases with consolidation pressure and with the degree of dispersion of a clay permeant system (Lambe, 1958; Mitchell, 1956; and Bolt, 1956).

Comparison of the possible and actual discrepancies.—Fig. 9 and 11 show that the principal features of the possible discrepancies due to tortuous flow paths are closely similar to those for high viscosity. Hence the previous discussion on high viscosity applies here to tortuous flow paths, and the result is immediately obtained that virtually none of the actual discrepancies can be explained by either factor. In addition, the actual discrepancies cannot be explained by a combination of the factors.

Additional evidence was obtained by Olsen (1961) which also shows that the failure of eq. (1) in saturated clays cannot be explained by tortuous flow paths. Kaolinite samples that had been consolidated one-dimensionally to maximum past pressures ranging from 4 to 256 atm, and illite Boston blue clay samples that had been consolidated to a maximum past pressure of over 200 atm, were subjected to tests in which the ratios of the flow rates in directions perpendicular and parallel to the direction of consolidation were determined. The ratios for all the kaolinite samples varied from 1.3 to 1.7. The ratios for the illite and Boston blue clay samples varied from 0.9 to 4.0.

For comparison with the above measured ratios, possible flow rate ratios that could be caused by the sole influence of tortuous flow paths were estimated from the model in Fig. 10. For kaolinite, assuming a particle axial ratio of to 10, the estimated flow rate ratios vary from 1 to about 20. For the other clays, assuming a particle axial ratio of to 20, the estimated flow rate ratios vary from 1 to about 100. The ratios of 1 are for random particle orientations. The high ratios are for complete particle orientation in the direction perpendicular to that of the consolidation pressure.

The large disagreement between the measured and estimated flow rate ratios precludes the possibility that the flow channels in clays are tortuous in some manner similar to that shown in Fig. 10, and substantiates the previous result that tortuous flow paths cannot be the principal cause for the failure of eq. (1) in clays.

Unequal Pore Sizes

An estimate was made of the discrepancies from eq. (1) that could arise owing to the sole influence of unequal pore sizes for the assumed condition that unequal pore sizes result from the grouping of clay particles in clusters. These estimated possible discrepancies are compared with the actual discrepancies obtained in the experimental investigation. With this comparison, the actual discrepancies are explained in terms of the cluster concept. Finally the cluster concept explanation is examined in respect to its compatibility with the electrical conductivity data.

Estimated possible discrepancies.—The possible discrepancies due to unequal pore sizes are herein defined by the ratio, q_5/q, where q_5 is the flow rate through a porous medium having unequal pore sizes, and q is the flow rate predicted from eq. (1).

The possible discrepancies were estimated from the assumptions that the factor, unequal pore sizes, is the sole cause for the failure of eq. (1) in saturated clays, and that unequal pore sizes are caused by the grouping of clay particles in clusters. A basis for estimating the possible discrepancies was obtained by deriving (Olsen, 1961) a relationship for flow rates through the cluster model shown in Fig. 12.

The model consists of clusters that are equidimensional, uniform in size, and porous. Three parameters define the model pore geometry: (1) N, the cluster mass, or the number of particles per cluster; (2) e_c, the intra-cluster void ratio; and (3) e_p, the inter-cluster void ratio, which equals the total void ratio minus the cluster void ratio, $e_T - e_c$. Consideration is given only to that component of flow passing through the large pores around and between the clusters. Since flow rates are proportional to the fourth power of pore radii, the contribution of that flow component through the cluster pores must be negligible.

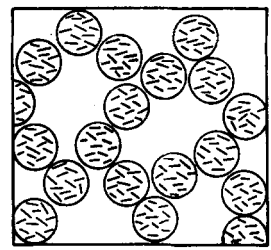

FIGURE 12.—Cluster model. Parameters: V_v = total void volume; V_s = total solids volume; V_c = volume of cluster voids; V_p = volume of voids between clusters; e_T = total void ratio = $\frac{V_v}{V_s}$ e_c = cluster void ratio = $\frac{V_c}{V_s}$; N = number of particles per cluster.

Equation (10) is the derived relationship for the flow rate, q_5, through the cluster model. Since it is given as the ratio, q_5/q, the equation also expresses the possible discrepancies from eq. (1) due to unequal pore sizes.

$$\frac{q_5}{q} = N^{2/3} \frac{[1 - e_c/e_T]^3}{[1 + e_c]^{4/3}}. \tag{10}$$

In order to estimate possible discrepancies with eq. (10) that could be compared with the actual discrepancies in Figs. 5 and 6, it was necessary to assume a relationship for the variations of the cluster void ratio, e_c, with changes in the total void ratio, e_T, that occur during compression and

https://doi.org/10.1346/CCMN.1960.0090108 Published online by Cambridge University Press

rebound. The assumed relationship, shown in Fig. 13, was chosen to conform with the following concepts concerning the relative compressibilities of the individual clusters and the cluster skeleton.

At high total void ratios, or porosities, the compressibility of the individual clusters is considered negligible compared to that of the cluster

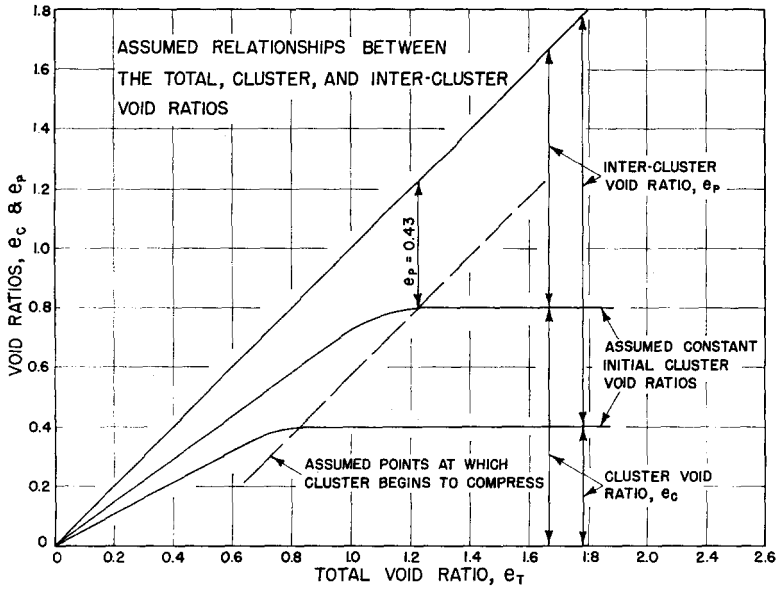

FIGURE 13.—Assumed relationships between the total, cluster and inter-cluster void ratios.

skeleton. During compression when the clusters approach a density corresponding to the densest possible packing of spheres, the clusters themselves begin to compress as the total void ratio is decreased. As the total void ratio approaches zero, both the cluster and the inter-cluster void ratios also approach zero.

Fig. 14 shows estimated possible discrepancies that were computed from eq. (10) together with the assumed relationships between the total and cluster void ratios shown in Fig. 13. Possible discrepancies are shown for a range of values for the initial cluster void ratio, e_{ci} and the cluster mass, N.

The additional assumptions needed to interpret Fig. 13 have been chosen from the following considerations. Dispersed, flocculated, and aggregated soil systems differ basically in respect to the magnitudes and signs of their interparticle forces. Dispersed systems have repulsive interparticle forces which tend to cause adjacent particles to align parallel to each other.

https://doi.org/10.1346/CCMN.1960.0090108 Published online by Cambridge University Press

Flocculated and aggregated systems have attractive interparticle forces which tend to cause less parallelism between particles, and which cause clustering in soil suspensions, some natural clays, and perhaps also dense pure clays.

From the above it appears reasonable to assume that the cluster mass, N, has a unique value for a specific soil permeant system, and that both the cluster mass and the initial cluster void ratio, e_{ci}, decrease with increasing dispersion of clay–permeant systems.

Comparison of the possible and actual discrepancies.—Figs. 5, 6 and 14 show that the principal features of the estimated possible discrepancies agree with those of the actual discrepancies. The extent of the agreement seems remarkably close, considering the simplicity of the assumptions on which the possible discrepancies were estimated.

At all porosities, the possible discrepancies cover the range of magnitudes of the actual discrepancies. Hence the cluster concept explains the fact that measured flow rates were sometimes less, and often considerably greater than those predicted from eq. (1).

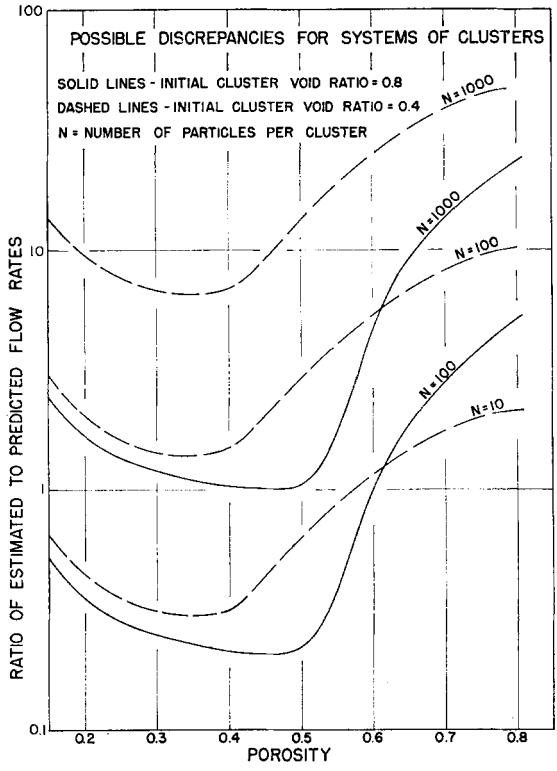

FIGURE 14.—Possible discrepancies for systems of clusters.

https://doi.org/10.1346/CCMN.1960.0090108 Published online by Cambridge University Press

The changes with porosity of the actual and possible discrepancies are similar over the entire porosity range. Since the porosity dependence of the estimated possible discrepancies results from the assumed relation between cluster and total void ratios, the porosity dependence of the actual discrepancies is explained by the concepts implied in Fig. 13, which are that (1) at high total porosities, consolidation is accompanied predominantly by cluster rearrangements and consequent changes in the inter-cluster component of void ratio, e_p; and (2) at low total porosities, consolidation and rebound are accompanied for the most part by compression and expansion of the clusters and consequently with relatively small changes in the inter-cluster void ratio, e_p.

Fig. 5 and 14 show that the actual and possible discrepancies also agree with respect to their dependence on the degree of dispersion of the clay–permeant systems. The actual discrepancies decrease with increasing dispersion; the possible discrepancies decrease with decreasing values of the cluster parameters, N and e_{ci}. The extent of this agreement is further examined below using the results from all clay–permeant systems tested in the consolidation–permeation tests.

Table 3 presents values for the cluster parameters that were computed from the experimental hydraulic flow data, the cluster flow equation (eq. 10), and the assumption that at high porosities the cluster void ratio, e_c, is a constant. For each clay the systems are listed in the order of increasing dispersion. With two exceptions the results show corresponding decreases in the values for the initial cluster void ratio, e_{ci}, the cluster mass, N, and the initial cluster diameter.

The exceptions do not indicate significant deviations from the above trends since they are easily explained by other factors. The anomalous parameter values for the 10^{-4} N Na-kaolinite system may be attributed to edge-to-face flocculation. The inconsistent results for the sodium Boston blue clay sample are explainable by the fact that some of the fines were lost during the centrifugation phase of its preparation procedure.

The unusually high values for the illite cluster parameters, compared with those for the kaolinites and Boston blue clays, also are easily explained according to the cluster concept. The illite was found to contain about 1.0 percent organic matter, and it is well known that organic matter is a potent aggregating agent in soils.

In summary, it has been shown that the discrepancies between measured and predicted flow rates (Figs. 2, 3 and 4) are fully explainable in terms of the cluster concept, as follows: (1) During consolidation at high porosities, the fact that measured flow rates decrease more rapidly than those predicted was accounted for by the rearrangement of clusters in the cluster skeleton such that the clay compression was accompanied predominantly by decreases in the size of the large pores surrounding the clusters. (2) During consolidation

TABLE 3.—CLUSTER PARAMETERS FROM HYDRAULIC DATA

Clay	Permeant	Initial Cluster Void Ratio e_{ci}	Particles per Cluster N	Initial cluster Diameter, d_{ci}, (μ)
Natural kaolinite	Distilled H_2O	0.53	83	1.06
Calcium kaolinite	10^{-1} N $CaCl_2$	0.50	34	0.78
Calcium kaolinite	10^{-3} N $CaCl_2$	0.50	28	0.73
Sodium kaolinite	10^{-1} N NaCl	0.45	17	0.61
Sodium kaolinite	10^{-3} N NaCl	0.40	9	0.49
Sodium kaolinite	10^{-4} N NaCl	0.45	14	0.57
Sodium kaolinite	0.02% sodium tetraphosphate (by weight)	0.40	7	0.48
Sodium kaolinite	1.0% sodium tetraphosphate (by weight)	0.30	3	0.33
Sodium illite	10^{-1} N NaCl	0.74	2150	0.34
Sodium illite	10^{-4} N NaCl	0.60	110	0.12
Calcium Boston blue clay	10^{-1} N $CaCl_2$	1.00	26	0.15
Calcium Boston blue clay	10^{-3} N $CaCl_2$	0.90	19	0.13
Sodium Boston blue clay	10^{-1} N NaCl	1.10	—	0.26

and rebound, respectively, at low porosities, the facts that measured flow rates decreased and increased less rapidly with porosity than those predicted were explained by attributing the primary seat of the volume changes to the clusters themselves; thereby providing that total porosity changes were accompanied predominantly by changes in the cluster void ratio, and with relatively small changes in the size of the larger liquid conducting pores surrounding the clusters. (3) Finally, the fact that at a given porosity measured flow rates vary with the chemical compositions of the clay and permeant was explained as being the result of the dependence of the cluster

mass and cluster void ratio parameters on the degree of dispersion of a clay permeant system; where both parameters decrease with increasing dispersion.

Electrical conductivity data.—The foregoing explanation for the actual discrepancies is herein examined with respect to its compatibility with the electrical conductivity data that were obtained in the experimental investigation. Use of the conductivity data provides an independent check on the cluster concept explanation, since the coupling between electrical and viscous flows was found to be negligible, and further since the flows of current and liquid in a pore follow different laws. In systems with highly conductive pore liquids, current is proportional to the square, whereas viscous flow is proportional to the fourth power, of the pore radius.

The electrical data are analyzed with a relationship that was derived for the conductivity of a clustered system. The data and relationships are used to evaluate the assumed constancy of cluster void ratios at high porosities, and to predict the cluster parameters for some of the clay systems. These parameters are then compared with those predicted from the hydraulic flow rate data.

A relationship for the conductivity of a clustered system was derived (Olsen, 1961) from the model shown in Fig. 12. Consideration was given to three current flow paths through the model: (1) through the large pores between the clusters; (2) through a path that alternately passes through and between the clusters; and (3) through a path that passes through the clusters at their points of contact. The contribution of the third path was ignored after finding it to be negligible when contact areas between the clusters are less than 10 percent. The relationship is

$$\sigma_T (1 + e_T) = \frac{\sigma_1}{T_1^2} (1 + x) (e_T - e_c), \tag{11}$$

where σ_T = total conductivity of clay,
σ_1 = specific conductivity of pore liquid,
T_1 = tortuosity of flow between clusters,
T_c = tortuosity of flow within clusters,
x = parameter dependent on e_T, e_c, T_1, and T_c.

Equation (11) rests on the assumption that the contribution of the excess ions in the electrical double layer to the conductivity is negligible. This condition can only hold in systems having highly conductive pore liquids, and hence only the data from systems having permeants and pore liquids with high ionic concentrations (10^{-1} N) are considered below.

For the following discussion a simple relationship is needed to describe the dependence of the parameter x on the total void ratio, e_T. An approximate relationship was obtained by calculating values of x using the assumed relationship between e_T and e_c shown in Fig. 13. The calculated results show (Olsen, 1961) that x remains a constant with changes in e_T at high

https://doi.org/10.1346/CCMN.1960.0090108 Published online by Cambridge University Press

total void ratios; and that x is approximately a constant over the entire porosity range provided that the ratio, T_c/T_1, is greater than about 5.

With the assumption that x remains a constant with changes in e_T for a given clay permeant system, eq. (11) can be used to examine the compatibility of the electrical conductivity data with the cluster concept explanation for the hydraulic flow rate results.

Equation (11) predicts that the term $\sigma_T(1 + e_T)$ will be linear with the total void ratio, e_T, at high porosities if the cluster void ratio remains constant. The corresponding experimental relationships were indeed found to be linear at high porosities for all the systems having pore liquid ionic concentrations of 10^{-1} N. The linearity can be seen for kaolinite samples in the typical results presented in Fig. 15.

Equation (11) may be used to obtain two cluster parameters from experimental relationships between σ_T $(1 + e_T)$ and e_T (*e.g.* the typical results in Fig. 15): (1) the initial and constant cluster void ratio, e_{ci}; and (2) the critical total void ratio, e_{Tc}, at which cluster compressions begin.

Equation (11) predicts that e_{ci} values are the intercepts on the e_T axes of the extrapolated linear relationship between the measured quantities, $\sigma_T(1 + e_T)$ and e_T. Also, with the assumption that the ratio T_c/T_1 is greater than 5, eq. (11) predicts that e_{Tc} values are the total void ratios at which the experimental $\sigma_T(1 + e_T)$ versus e_T relationships cease to be linear.

The cluster parameter values for all the systems having pore liquid ionic concentrations of 10^{-1} N were thus obtained. The results are listed in Table 4, together with corresponding parameter values that were obtained from the hydraulic flow rate data.

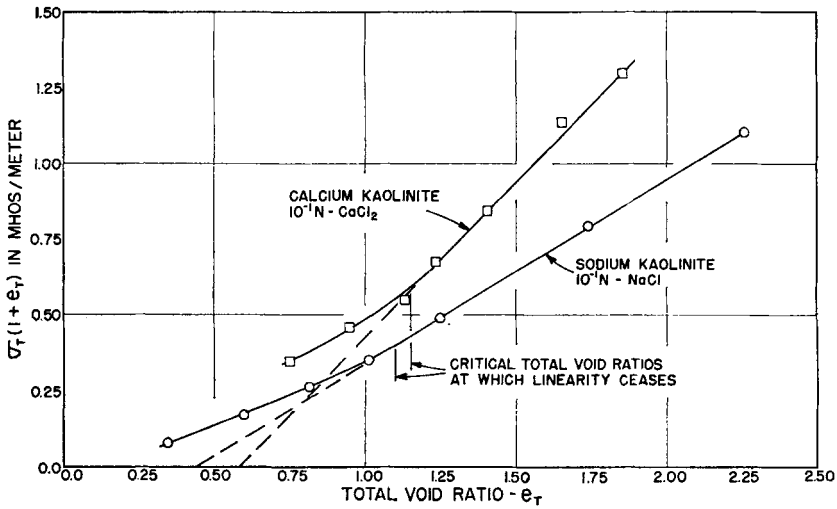

FIGURE 15.—Relationship between $\sigma_T(1 + e_T)$ and total void ratio.

https://doi.org/10.1346/CCMN.1960.0090108 Published online by Cambridge University Press

The close agreement between the hydraulic and electrical parameters indicates that the electrical conductivity data are compatible with the same cluster concept that was used to explain the discrepancies between the measured and predicted hydraulic flow rates.

The validity of the foregoing analysis may seem questionable owing to the assumption of negligible surface conductance that was used in the derivation of eq. (11). That surface conductance is often important in clays is well known. Therefore, it is necessary to consider the extent to which the analysis depends on the assumption of negligible surface conductance.

Only one aspect of the behavior predicted by eq. (11) was used in the analysis; namely, the predicted linearity of $\sigma_T(1 + e_T)$ *vs.* e_T for constant values of e_c. For this aspect to be linear it is required only that surface conductance be negligible in the large pores, since variations in e_T are accompanied only by changes in the large pore volume. Hence the validity of the analysis requires that surface conductance be negligible only in the large pores.

TABLE 4.—COMPARISON OF CLUSTER PARAMETERS FROM HYDRAULIC AND ELECTRICAL DATA

Clay	Permeant	Initial Cluster Void Ratios		Critical Total Void Ratios at which Clusters begin to Compress	
		Hydraulic data	Electrical data	Hydraulic data	Electrical Data
Sodium kaolinite	10^{-1} N NaCl	0.45	0.43	1.05	1.10
Calcium kaolinite	10^{-1} N $CaCl_2$	0.50	0.57	1.15	1.15
Sodium Boston blue clay	10^{-1} N NaCl	1.10	1.18	2.25	2.20
Calcium Boston blue clay	10^{-1} N $CaCl_2$	1.00	1.05	2.35	2.30
Sodium illite	10^{-1} N NaCl	0.74	0.62	1.60	1.53

Discussion.—The critical concepts in the foregoing cluster explanation for the discrepancies between measured hydraulic flow rates and those predicted from Darcy's law and the Kozeny–Carman equation are: (1) the clay pores are not equal in size and nearly all of the flow passes through only that part of the clay porosity that is distributed among the larger pores; (2) at high porosities, compression of the clay is accompanied predominantly by a decrease in size of the large pores; and (3) at very low porosities the volume changes of the clay are accompanied for the most part by changes in the porosity that is distributed among the smaller pores.

https://doi.org/10.1346/CCMN.1960.0090108 Published online by Cambridge University Press

It seems likely that other models which incorporate these critical concepts may also provide satisfactory explanations for the discrepancies; for example, honeycomb, packet, domain, or fissure models of clay structure. It is not difficult to imagine ways for the components of porosity in these models to vary so that their relationships with changes in total porosity are in accord with the above critical concepts in the cluster explanation.

Thus it appears that the success of the cluster explanation does not necessarily indicate that the clay consists of a clustered structure; it does, however, point to the existence of unequal pore sizes as the principal cause for the failure of eq. (1) in clays.

SUMMARY AND CONCLUSIONS

Hydraulic flow rates, electrical conductivities, and streaming potentials were measured on natural, sodium, and calcium samples of kaolinite, illite and Boston blue clay. Data were taken after increments of one-dimensional consolidation and rebound over the pressure range from one-sixteenth to 256 atm. The discrepancies between the measured flow rates and those predicted from Darcy's law and the Kozeny–Carman equation were calculated. The magnitudes of the discrepancies, their dependence on porosity, and their variations with the chemical compositions of the clays and permeants were determined.

Analyses then were made of the extent to which the discrepancies can be explained by each of the following: (1) possible errors in Darcy's law, (2) electrokinetic coupling, (3) high viscosity, (4) tortuous flow paths, and (5) unequal pore sizes.

The validity of Darcy's law was discussed in light of recent evidence that suggests it is violated at low pressure gradients. The discrepancies that could arise owing to the possible errors in Darcy's law were found to be insignificant compared with the actual discrepancies.

The influences of electrokinetic coupling on the measured flow rates were computed from irreversible thermodynamic relationships together with the experimental data on hydraulic flow rates, electrical conductivities, and streaming potentials. The influences of electrokinetic coupling were found to be insignificant compared with the actual discrepancies.

The analyses for high viscosity and tortuous flow paths were similar. For each factor, an estimate was made of the discrepancies that it could cause from eq. (1). Using a comparison of the estimated possible discrepancies with the actual discrepancies, it was found that practically none of the actual discrepancies can be accounted for with high viscosity or tortuous flow paths.

The discrepancies that could arise from eq. (1) owing to unequal pore sizes were estimated for the assumed condition that unequal pore sizes

occur as a result of the grouping of clay particles in clusters. With the aid of a comparison of these estimated possible and the actual discrepancies, the actual discrepancies were fully explained in terms of the cluster concept. The cluster concept was further found to be compatible with the electrical conductivity data. Finally, it was pointed out that the success of the cluster concept explanation rests on its provision for unequal pore sizes in a clay; and that other models providing for unequal pore sizes, such as packets or domains, probably will explain the data as well.

The foregoing analyses lead to the conclusion that, for the saturated clays used in this investigation, the discrepancies between measured hydraulic flow rates and those predicted from Darcy's law and the Kozeny–Carman equation are caused primarily by unequal pore sizes in the clays.

REFERENCES

Bolt, G. H. (1956) Physical-chemical analysis of the compressibility of pure clay: *Geotechnique*, v. 6, no. 2, pp. 86–93.

Carman, P. C. (1956) *Flow of Gases Through Porous Media*: Academic Press, Inc., New York, 182 pp.

de Groot, S. R. (1959) *Thermodynamics of Irreversible Processes*: North Holland Publishing Co., Amsterdam, 242 pp.

Denbigh, K. G. (1951) *The Thermodynamics of the Steady State*: Methuen, Ltd., London; John Wiley & Sons, Inc., New York, 103 pp.

Elton, G. A. H. (1948) Electroviscosity: *Proc. Roy. Soc.*, v. 194A, pp. 259–287.

Guggenheim, E. A. (1957) *Thermodynamics*: North Holland Publishing Co., Amsterdam, 476 pp.

Hansbo, S. (1960) Consolidation of clay, with special reference to influence of vertical sand drains: *Swedish Geotechnical Institute Proceedings*, no. 18, pp. 41–61.

Lambe, T. W. (1954) The permeability of fine grained soils: *A.S.T.M. Special Publication 163*, pp. 56–67.

Lambe, T. W. (1958) The engineering behavior of compacted clay: *Proc. Amer. Soc. Civil Eng.*, v. 84, no. SM 2, 35 pp.

Loudon, A. G. (1952) The computation of permeability from simple soil tests: *Geotechnique*, v. 3, pp. 165–183.

Low, P. F. (1960) Viscosity of water in clay systems: in *Clays and Clay Minerals*, Pergamon Press, New York, v. 8, pp. 170–182.

Lutz, J. F. and Kemper, W. D. (1959) Intrinsic permeability of clay as affected by clay–water interaction: *Soil Sci.*, v. 88, pp. 83–90.

Macey, H. H. (1942) Clay en dash water relationships and the internal mechanism of drying: *Trans. Brit. Ceram. Soc.*, v. 41, pp. 73–121.

Michaels, A. S., and Lin, C. S. (1954) The permeability of kaolinite: *Ind. Eng. Chem.*, v. 46, pp. 1239–1246.

Michaels, A. S. (1959) Discussion of physical-chemical properties of soils. Soil water systems: *Proc. Amer. Soc. Civil Eng.*, v. 85, no. SM 2, pp. 91–102.

Mitchell, J. K. (1956) The importance of structure to the engineering behavior of clay: Sc. D. Thesis, M.I.T.

Olsen, H. W. (1961) Hydraulic flow through saturated clays: Sc. D. Thesis, M.I.T.

Quirk; J. P. (1959) Permeability of porous media: *Nature*, v. 183, pp. 387–388.

Quirk, J. P., and Schofield, R. K. (1955) The effect of electrolyte concentration on soil permeability: *J. Soil Sci.*, v. 6, pp. 163–178.

Terzaghi, C. (1925) Determination of permeability of clay: *Eng. News Record*, v. 95, pp. 832–836.

Von Englehardt, W. and Tunn, W. L. M. (1955) The flow of fluids through sandstones: *Illinois State Geological Survey Circular* 194 (translated by Witherspoon, P. A.).